Verification of Video Reconstruction Using Bilateral-Reverse Directional Global Based Optical Flow over Non-Gaussian Noise

Darun Kesrarat

Vincent Mary School of Science and Technology
Department of Information Technology
Assumption University, Bangkok, Thailand
Email: darunksr@gmail.com

Vorapoj Patanavijit

Vincent Mary School of Engineering
Department of Computer and Network Engineering
Assumption University, Bangkok, Thailand
Email: patanavijit@yahoo.com

***Abstract* - This paper presents the verification of video reconstruction over non-Gaussian noise using Bilateral-reverse directional global based optical flow. Noise is a major problem in optical for motion approximation where the effective result in motion vector (MV) is a core matter in the optical flow. Various type of noise cause the uncertain determination in the optical flow technique. Many of robust optical flow techniques were invented to increase the certainty of optical under noisy conditions. In our experimentation, we verified several of robust optical flow techniques with the Bilateral-reverse directional technique. The contaminated video with non-Gaussian noises is used to verify the performance on several robust optical flow techniques by considering the result in the video reconstruction from the MV on each technique to prove the robustness of Bilateral-reverse directional technique on global based optical flow.**

Keywords – Verification, Video Reconstruction, Bilateral-Reverse, Optical Flow, Non-Gaussian Noise

I. INTRODUCTION

In optical flow, 2-dimension of motion sequence is used to determine the MV. There are a variety of optical flow techniques such as global based [1], local based [2], and phase based [3]. Because of the advantage in the real-time computation of global-based optical flow technique, it is very favorite and it is used in several applications such as moving object tracking [4], video compression and encoding [5], and etc. But the global-based optical flow (GBOF) is very weak against noise.

Then, several of robust techniques were invented to increase the certainty outcome in GBOF technique. But, under several types of noises intersect with the different characteristics of video (image intensity and speed video of movement) lead to the difficulty for identifying the best robustness technique for GBOF. Some techniques present very well robustness under some types of noise or under some characteristics of video while the others present better robustness in the other condition. By the way, the consequence of application that applies the GBOF as a pre-process is also an issue of concern.

In this paper, we concern on the video reconstruction as the main issue where it uses the result MV of GBOF for image sequence reconstruction as a video. Basically, it is a part of video compression, video encoding, or super image reconstruction [6]. Then, we used Peak Signal to Noise Ratio (PSNR) to be a verification indicator with the regular ground truth video. We verified Bilateral-reverse directional technique (B-R) [7] against with the other robust techniques on GBOF. There are regular reverse directional certainty algorithm [8], and regular bilateral filter [9-11]. For non-Gaussian noise, we adapted Speckle Noise, Poisson Noise, and Salt&Pepper Noise with several characteristics of video for robustness verification.

Three more sections are included in this paper. There are 'Overview of optical flow and robust technique', 'Experimental verification', and 'Conclusion'.

II. OVERVIEW IN OPTICAL FLOW AND ROBUST TECHNIQUES

A. Global-based Optical Flow (GBOF)

The global-based differential technique assumes the minimization process by weighted average to solve the equation from spatiotemporal of image gradient (G) with four-point mean differences (1/12 [-1 : 8 : 0 : -8 : 1]) [12].

$$\begin{aligned} Gx&=1/12\{-Gx,y-2+ 8\times Gx,y-1+ -8\times Gx,y+1+Gx,y+2 \} \\ Gy&=1/12\{-Gx-2,y+8\times Gx-1,y+-8\times Gx+1,y+Gx+2,y \} \\ Gi&=1/12\{-Gx,y,i-2+8\times Gx,y,i-1+-8\times Gx,y,i+1+Gx,y,i+2 \} \end{aligned} \quad (1)$$

where G(x,y,i) implies the gradient tension (luminosity) in position (x,y) on the image at time i. The MV (u, v) of GBOF is computed by the iterative minimization process.

$$u^{h+1} = \bar{u}^h - \frac{G_x\left[G_x\bar{u}^h + G_y\bar{v}^h + G_i\right]}{\alpha^2 + G_x^2 + G_y^2}$$

$$v^{h+1} = \bar{v}^h - \frac{G_y\left[G_x\bar{u}^h + G_y\bar{v}^h + G_i\right]}{\alpha^2 + G_x^2 + G_y^2} \quad (2)$$

where α is smoothness weight. and are neighborhoods average.

Often GBOF presents very fast in computation but varies in the accuracy with the appropriated value of α.

B. Reverse Directional Certainty (RC)

Reverse directional certainty is an enhanced algorithm for the optical flow. RC consider the result of MV on reverse direction to measure the higher certainty defined as:-

$$C_d^n(x,y) = \exp\left(-\frac{|v_d^n(x,y)+v_{d^-}^n(x+v_d^n(x,y),y+1)|}{(|v_d^n(x,y)|+|v_{d^-}^n(x+v_d^n(x,y),y+1)|)/2+\beta}\right) \tag{3}$$

where C is certainty rate, β evades the dividing by zero in the prescription, d and d^- are common direction and reverse direction MV. The certainty will be rated to one when the results MV in both directions are balanced.

Next, the result MV of RC is solved by the mean MV in corresponded certainty rate of the neighborhood ($N(x_0)$) defined as:-

$$\bar{v}_d^n(x_0) = \left(\sum_{x_j \in N(x_0)} C_d^n(x_j)\, v_d^n(x_j)\right) \Big/ \left(\sum_{x_j \in N(x_0)} C_d^n(x_j)\right) \tag{4}$$

From the performance evaluation under fair and noisy condition [13,14], RC presents the impressive result in MV but the high computation is presented in return from the common algorithm. Then, this algorithm may not suitable for processing in real time motion approximation.

C. Bilateral Filter (BF)

Bilateral filter is an enhanced non-linear function and it is identified as an edge-preservation noise-overthrow by using averagely weighted from neighbors. BF for motion approximation is recognized as a smoothing filter in optical flow defined as:-

$$v_b(x) = \frac{1}{N}\sum_{|h|<H} v(x)\phi(x+H) \tag{5}$$

where H is the neighborhood's dimension. In our experiment, we rank H in ±7 according to the traditional scheme. N is the normalization kernel factor, it is defined as:-

$$N = \sum_{|h|<H} \phi(x+h) \tag{6}$$

The Gaussian kernel of bilateral (ϕ()) is defined as:-

$$\phi(x+h) = \exp\left(\frac{|h|^2}{2\delta_a^2} + \frac{|G(x+h)-G(x)^2|}{2\delta_b^2}\right) \tag{7}$$

where δb is image intensity G(x)'s standard deviation and δa is signal v(x) × 7's standard deviation.

D. Bilateral-Reverse Directional Technique (B-R)

B-R is a fusion technique using RC correspondent with BF on GBOF. According to the original framework of B-R [7], it presented very well performance over Additive White Gaussian Noise. The process flow of B-R is illustrated in Figure1.

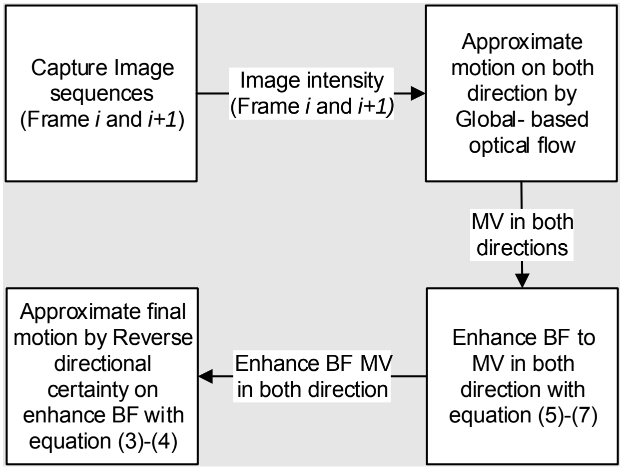

Figure 1: Process flow of B-R

III. EXPERIMENTAL FOR VERIFICATION

We verify the video reconstruction by using 4 standard recognizable videos (FOREMAN, CONTAINER, COASTGUARD, and AKIYO) in QCIF format (176×144) intersect with 3 forms of non-Gaussian noise (Speckle at variance 0.01-0.05, Poisson, and Salt&Pepper at density - 0.005-0.025). The characteristic of non-Gaussian noise in our experiment is illustrated in Figure2.

Then, totally 20 videos (100 frames on each) are used to verify the performance of video reconstruction in our experiment.

PSNR is used to determine the performance of video reconstruction by comparing with the ground truth video.

Figure3 to Figure 6 illustrate the PSNR graph in the scale of dB on the frame by frame basis from the performance of video reconstruction of each algorithm.


(a) Original Image


(b) Poisson

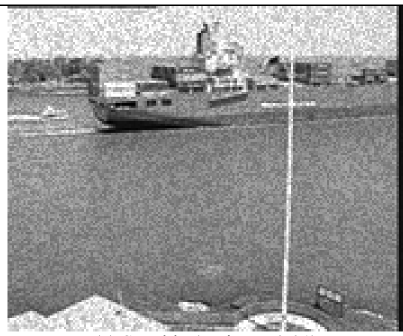
(c) Speckle (variance 0.01)

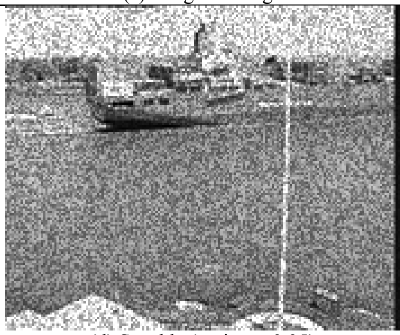
(d) Speckle (variance 0.05)


(e) Salt & Pepper (density 0.005)


(f) Salt & Pepper (density 0.025)

Figure 2: Image frame of contaminated non-Gaussian noises.

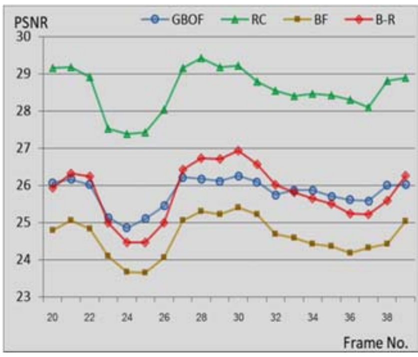

–a. Speckle (variance 0.01)

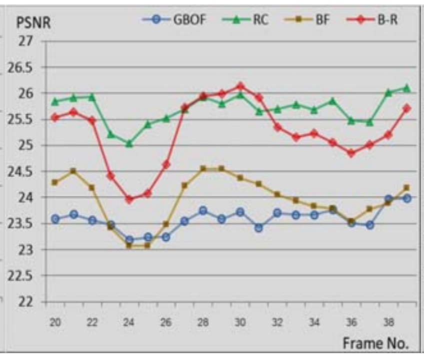

-b. Speckle (variance 0.05)

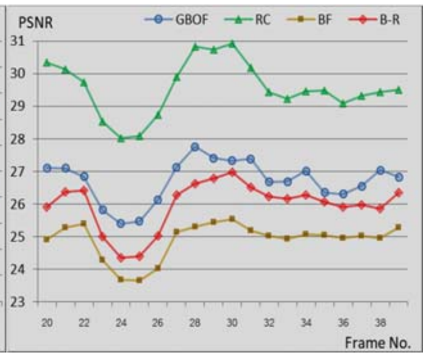

–c. Poisson

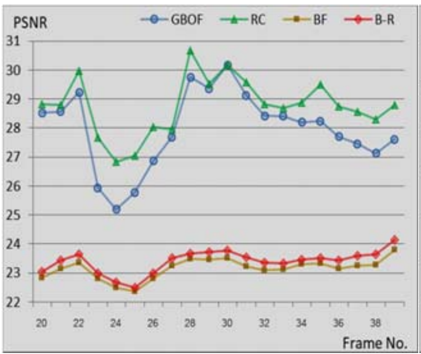

–d. Salt&Pepper (density 0.005)

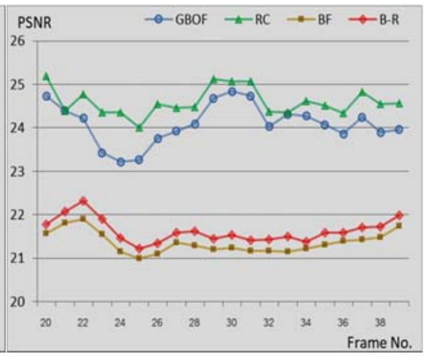

-e. Salt&Pepper (density 0.025)

Figure3: PSNR in consecutive frame no. 20-40 of FOREMAN video at distinctive noise

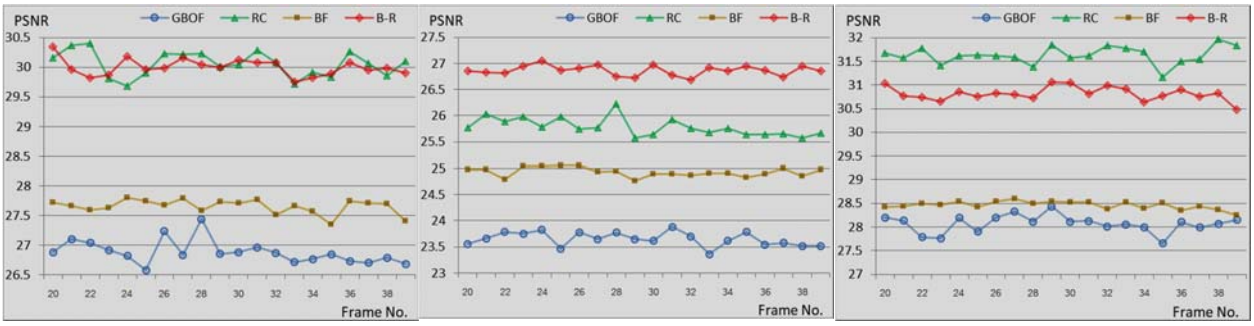

–a. Speckle (variance 0.01) -b. Speckle (variance 0.05) –c. Poisson

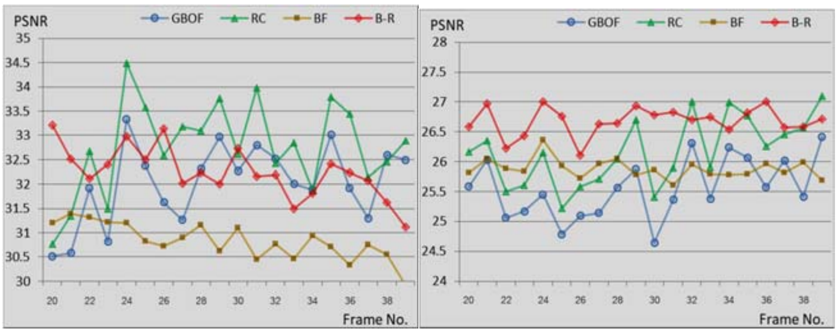

–d. Salt&Pepper (density 0.005) -e. Salt&Pepper (density 0.025)

Figure 4: PSNR in consecutive frame no. 20-40 of CONTAINER video at distinctive noise

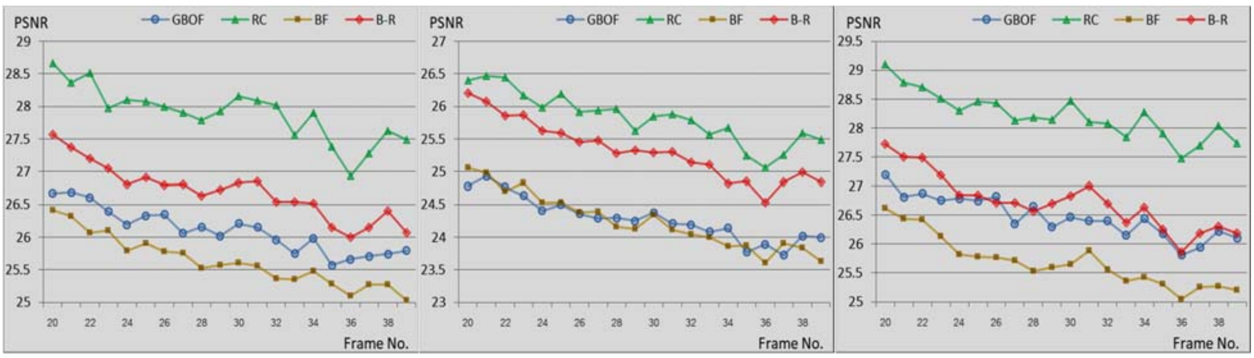

–a. Speckle (variance 0.01) -b. Speckle (variance 0.05) –c. Poisson

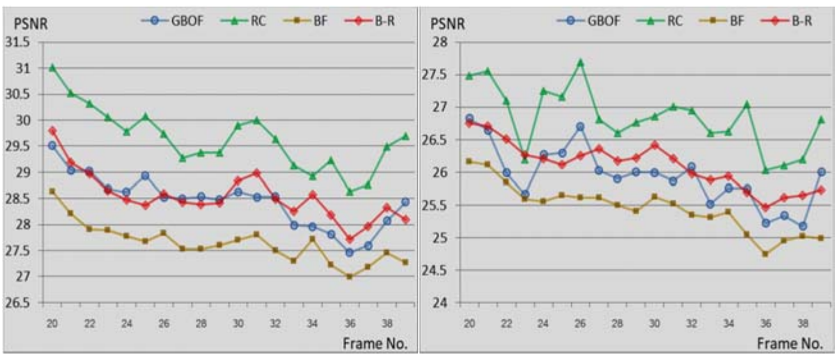

–d. Salt & Pepper (density 0.005) -e. Salt & Pepper (density 0.025)

Figure 5: PSNR in consecutive frame no. 20-40 of COASTGUARD video at distinctive noise

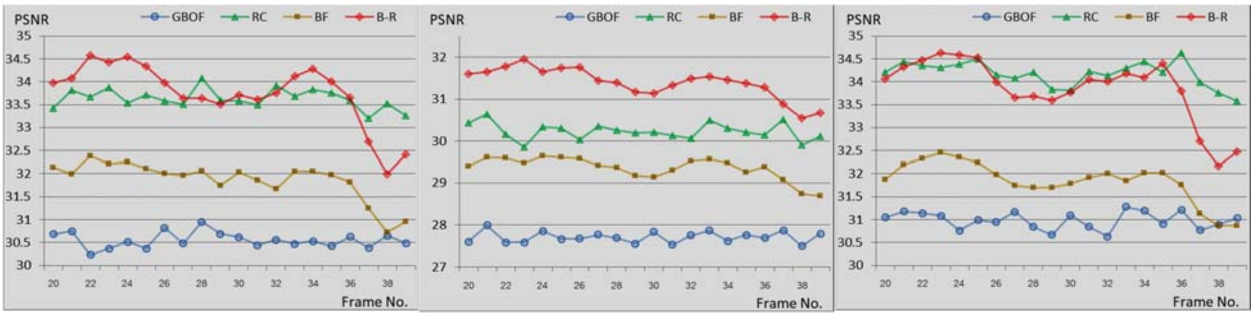

–a. Speckle (variance 0.01) -b. Speckle (variance 0.05) –c. Poisson

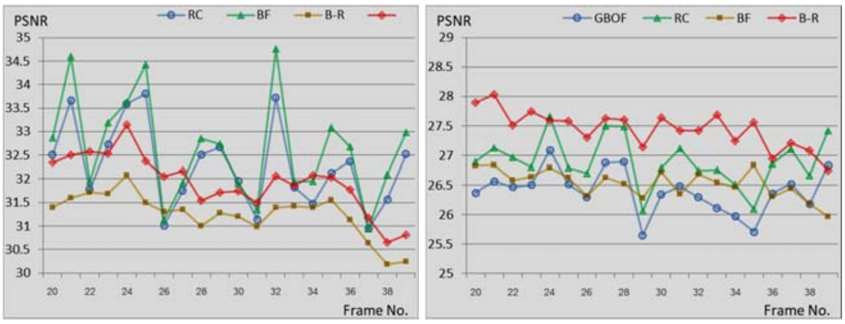

–d. Salt & Pepper (density 0.005) -e. Salt & Pepper (density 0.025)

Figure6: PSNR in consecutive frame no. 20-40 of AKIYO video at distinctive noise

And the average PSNR with SD over 100 consecutive frames of each video is briefed in Table1.

TABLE 1: AVERAGE PSNR AND SD FROM THE EXPERIMENT

		FOREMAN		CONTAINER		COASTGUA.		AKIYO	
		AVG PSNR (dB)	SD	AVG PSNR (dB)	SD	AVG PSNR (dB)	SD	AVG PSNR (dB)	SD
SPECKLE (variance 0.01)	GBOF	25.90	0.57	26.88	0.17	25.55	1.63	30.63	0.27
	RC	**28.45**	0.91	**30.02**	0.24	**27.23**	2.10	**33.78**	0.39
	BF	25.06	1.04	27.70	0.19	24.32	2.52	31.82	0.49
	B-R	26.12	1.31	29.98	0.28	25.29	2.86	33.75	0.72
SPECKLE (variance 0.05)	GBOF	23.67	0.42	23.68	0.14	23.67	1.31	27.69	0.19
	RC	**25.63**	0.64	25.75	0.20	**25.14**	1.63	30.19	0.23
	BF	24.15	0.77	25.08	0.17	23.34	2.01	29.15	0.42
	B-R	25.35	1.02	**27.00**	0.17	24.32	2.29	**31.08**	0.66
POISSON	GBOF	26.73	0.70	28.03	0.22	25.83	1.74	30.98	0.24
	RC	**29.28**	1.06	**31.54**	0.23	**27.55**	2.21	**34.27**	0.36
	BF	25.32	1.11	28.66	0.32	24.50	2.56	32.10	0.50
	B-R	26.23	1.36	31.06	0.36	25.46	2.91	34.05	0.75
SALT&PEPPER (density 0.005)	GBOF	27.79	1.32	31.61	0.93	27.69	2.60	32.03	0.86
	RC	**28.42**	1.27	**32.22**	1.13	**28.72**	2.89	**32.41**	1.01
	BF	24.59	1.49	31.01	0.47	25.46	3.40	32.00	1.00
	B-R	24.89	1.59	32.12	0.70	26.17	3.79	32.77	1.19
SALT&PEPPER (density 0.025)	GBOF	24.15	0.57	25.53	0.51	25.29	1.82	26.33	0.44
	RC	**24.64**	0.55	26.17	0.58	**26.09**	1.99	26.80	0.51
	BF	22.34	1.00	26.10	0.54	23.86	2.48	26.87	0.65
	B-R	22.72	1.15	**27.03**	0.76	24.42	2.69	**27.72**	0.81

IV. CONCLUSIONS

From the experimental, the non-Gaussian noise impacts the global-based optical flow as the result that the value of PSNR on reconstructed video is dropped. The different results in performance are returned under the different form of non-Gaussian noises and the different characteristic of the video.

In the overall B-R and RC present the best and the second best result for the video reconstruction from global-based optical flow under non-Gaussian noises.

The B-R presents the best result under SPECKLE noise and SALT&PEPPER noise at the high level of noise on CONTAINER and AKIYO sequences while RC presents the best result over low noise level.

RC also presents the best result under POISSON noise and low noise level of SPECKEL and SALT&PEPPER noise on all sequences following by B-R.

The characteristic of CONTAINER and AKIYO sequences is a quite slow movement while the characteristic of FOREMAN and COASTGUARD sequences is fast movement. Then, we concluded that the B-R is very well effective on enhancing the global-based optical flow under the slow movement sequence under the high level of non-Gaussian noises.

ACKNOWLEDGMENT

This research project was funded by Assumption University.

REFERENCES

[1] B.K.P. Horn and B.G. Schunck, "Determining Optical Flow," Artificial Intelligence, vol. 17, pp. 185-203, 1981.

[2] B.D. Lucas and T. Kanade, "An Iterative Image Registration Technique with an Application to Stereo Vision, " In proceeding of Defense Advanced Research Projects Agency (DARPA) Image Understanding Workshop, pp. 121-130, 1981.

[3] D.J. Fleet and A.D. Jepson, "Computation of component image velocity from local phase information," Computer Vision 5, pp.77-104, 1990.

[4] S.A. Mahmoudi, M. Kierzynka, P. Manneback, and K. Kurowski, "Real-time motion tracking using optical flow on multiple GPUs," Bull. Pol. Ac.:Tech., vol.62 (1), pp.139-150, 2014.

[5] "Draft ITU-T Rec. and Final Draft International Standard of Joint Video Specification (ITU-T Rec. H.264-ISO/IEC 14 496-10 AVC)," Joint Video Team (JVT) of ISO/IEC MPEG and ITU-T VCEG, document JVT-G050r1.doc, JVT of ITU-T and ISO/IEC JTC1, (2003)

[6] M. Liang, J. Du, and H. Liu, "Spatiotemporal Super-Resolution Reconstruction Based on Robust Optical Flow and Zernike Moment for Video Sequences, " Mathematical Problems in Engineering , vol. 2013, pp.1-13, 2013.

[7] D. Kesrarat and V. Pattanavijit, "Robust Global Based Spatial Correlation Optical Flow in Bidirectional Confidential Technique with Bilateral Filter", International Conference on Intelligent Informatics and BioMedical Sciences (ICIIBMS 2015), pp. 1-4, 2015.

[8] R. Li and S. Yu, "Confidence Based Optical Flow Algorithm for High Reliability," In proceeding of IEEE International Conference on Acoustics, Speech, and Signal Processing (ICASSP), pp. 785-788, 2008.

[9] J.Sun, Y. Li, S. Kang, and H.-Y. Shun, "Symmetric stereo matching for occlusion handling," In proceeding of IEEE Conf. Comput. Vis.Pattern Recognit., pp. 399-406, 2005.

[10] S. Paris, P. Kornprobst, J. Tumblin, and F. Durand, "Bilateral filtering: Theory and Applications," Found. Trends Compt. Graph. Vis., Vol.4, No.1, pp.1-73, 2008.

[11] M. G. Mozerrov, "Constrained Optical Flow Estimation as a Matching Problem," IEEE Transactions on Image Processing, Vol.2, No.5, pp. 2044-2055, 2013.

[12] J.L. Barron, D.J. Fleet, and S.S. Beauchemin, "Performance of Optical Flow Techniques," International Journal of Computer Vision, Vol. 12, pp. 43-77, 1994.

[13] D. Kesrarat and V. Patanavijit, "Experimental Performance Analysis of High Confidence Reliability Based on Differential Optical Flow Algorithms over AWGN Sequences with Sub-Pixel Displacement," In proceeding of IEEE Intelligent Signal Processing and Communications Systems (ISPACS), pp. 1-6, 2011.

[14] D. Kesrarat, P. Porntrakoon and V. Patanavijit, "Investigation of Performance Trade off in High Reliability and Robust Gradient Orientation on Differential Sub-Pixel Displacement Optical Flow Algorithms over Non Gaussian Noisy Model," In proceeding of IEEE Electrical Engineering/Electronics, Computer, Telecommunications and Information Technology (ECTI-CON), pp. 1-4, 2012.